

Simultaneous electrochemical immunosensing of alpha-fetoprotein and prostate specific antigen using a glassy carbon electrode modified with gold nanoparticle-coated silica nanospheres and decorated with Azure A or ferrocenecarboxylic acid

Junqing Zhao¹ · Zilin Guo¹ · Dexiang Feng^{1,2} · Jinjin Guo¹ · Junchun Wang¹ · Yuzhong Zhang¹

Received: 28 April 2015 / Accepted: 1 August 2015 / Published online: 11 August 2015
© Springer-Verlag Wien 2015

Abstract We describe an electrochemical immunosensor for the simultaneous determination of alpha-fetoprotein (AFP) and prostate specific antigen (PSA) via a modified glassy carbon electrode. Silica nanoparticles (200–300 nm i.d.) with good monodispersity and uniform shape were synthesized, and the following species were then consecutively immobilized on their surface: gold nanoparticles (AuNPs; 5–15 nm i.d.), secondary antibody (Ab₂) and the redox-probes Azure A or ferrocenecarboxy acid (Fc). In parallel, two types of primary antibodies (Ab₁) were co-immobilized on the surface of the dissolved reduced graphene oxide sheets (rGO) that were also decorated with AuNPs. In the presence of antigens (AFP or PSA), the Ab₂/Si@AuNPs carrying Azure A and Fc are attached to the AuNP/rGO conjugate via a sandwich type immunoreaction. Differential pulse voltammetry (DPV) was employed to measure the resulting changes in the signal of Fc or Azure A. Two well-resolved oxidation peaks, one at –0.48 V (corresponding to Azure A) and other

at +0.12 V (corresponding to Fc; both vs. SCE) can be observed in the DPV curves. Under optimal conditions, AFP and PSA can be simultaneously determined in the range from 0.01 to 25 ng mL⁻¹ for AFP, and from 0.012 to 25 ng mL⁻¹ for PSA. The detection limits are 3.3 pg mL⁻¹ for AFP and 4.0 pg mL⁻¹ for PSA (at a signal-to-noise ratio of 3). The method was applied to (spiked) real sample analysis, and the recoveries are within 96.0 and 107.2 % for PSA, and within 100.9 and 105.8 % for AFP, indicating that this dual immunosensor matches the requirements of clinical analysis.

Keywords Electrochemical immunosensor · Silica nanoparticles · Gold nanoparticles · Azure A · Ferrocenecarboxylic acid · Differential pulse voltammetry · Immunosensor

Introduction

The prostate specific antigen (PSA), a single chain glycoprotein with a molecular weight of 32–33 kDa, is a reliable and widely used tumor biomarker [1]. For healthy individuals, the PSA concentration in serum is below 4 ng mL⁻¹, and higher level is related to prostate cancer [2]. Alpha-fetoprotein (AFP) is another widely used tumor biomarker, its normal level in serum is less than 25 ng mL⁻¹, and higher level is related to liver cancer [3]. Thus, monitoring the level of PSA or AFP is very helpful for clinical diagnosis. However, most biomarkers are not specific to a particular tumor. For example, AFP is associated with liver cancer and epithelial ovarian tumors, while carcinoembryonic antigen (CEA) is associated with colorectal cancer, liver cancer and pancreatic cancer. The result

Electronic supplementary material The online version of this article (doi:10.1007/s00604-015-1591-8) contains supplementary material, which is available to authorized users.

✉ Yuzhong Zhang
zhyz65@mail.ahnu.edu.cn

¹ College of Chemistry and Materials Science, the Key Laboratory of Functional Molecular Solids, Ministry of Education, Anhui Laboratory of Molecule-Based Materials, Anhui Key Laboratory of Chem-Biosensing, Anhui Normal University, Wuhu 241000, People's Republic of China

² Department of Chemistry, Wannan Medical College, Wuhu 241002, People's Republic of China

from single biomarker detection tends to provide false information. Moreover, most cancers exhibit an elevation of the level of two biomarkers at least. So, simultaneous detection of multiple biomarkers related to a certain cancer in a single run has attracted considerable attention [4, 5].

Various methods have been reported to realize multiple biomarkers detection including enzyme-linked immunosorbent assay, chemiluminescence immunoassay, fluorescence immunoassay, electrochemical immunoassay, electrochemiluminescence immunoassay [6–8]. Among them, electrochemical immunosensor has become one of the promising techniques due to its advantages such as high sensitivity, high selectivity and simple instrument. To date, various immunosensors have been reported for the detection of biomarkers based on enzyme [9], quantum dots (QD) [10–12] and dye-doped nanoparticles amplifying detection signal [13, 14]. For multiple biomarkers detection, the major problem is how to obtain and discriminate every signal of the corresponding biomarker. From literature, we have known multi-labelled strategy is a good approach to solve the problem. For instance, different metal sulfide nanoparticles were used as signal tags to label secondary antibody (Ab_2), and distinguishable peaks were obtained in anodic stripping voltammograms [15]. Other, various redox probes (e.g., Prussian blue, thionine, ferrocene etc.) were used to label Ab_2 , and the well-resolved peaks were obtained in DPV curves [16–18]. Compared with metal nanoparticles markers, the redox-probes show many advantages such as shorter time and do not require harsh conditions including acid dissolution step and high potential accumulation. However, the problem of this method is to find suitable redox-probes whose signals do not overlap each other.

Based on the advantages of redox probe, we have designed an electrochemical immunosensor for multiple biomarkers detection. Previously, we had described an electrochemical immunosensor for the simultaneous detection of CEA and AFP based on redox probe labeling signal antibody [19]. In design, thionine and prussian blue were employed to label Ab_2 , reduced graphene oxide (rGO) was used for the immobilization of primary antibodies (Ab_1), the immunosensor obtained can permit simultaneous detection of CEA and AFP in a single run. In present study, Azure A and ferrocenecarboxylic acid (Fc), whose signals can be distinguished clearly, were selected to label Ab_2 via the carboxyl or amino group. In order to improve the immobilized amount of Ab_2 and redox-probe, Silica nanoparticles (Si NPs) and gold nanoparticles (Au NPs), with a larger surface and good biocompatibility, were employed to immobilize Ab_2 (Ab_2 /Si@Au NPs) and redox-probe; Au NPs decorated rGO (Au NPs/rGO) nanomaterial, with a larger surface and good conductivity, were used for two different Ab_1 immobilization. In the presence of AFP and PSA, redox-probes coated Ab_2 /Si@Au NPs were captured onto the surface of Au NPs/rGO

via the immunoreaction. The responsive signal from Fc and Azure A were clearly distinguished in different pulse voltammograms. So, this immunosensor can detect AFP and PSA simultaneously in a single run. Because of the use of Si@Au NPs and rGO in sensing system, the responsive signals are clearly increased. As a result, the immunosensor exhibits high sensitivity.

Experimental

Chemicals and reagents

Alpha-fetoprotein (AFP), AFP antibody (anti-AFP), prostate specific antigen (PSA), monoclonal PSA antibody (anti-PSA) and human chorionic gonadotropin (HCG) were purchased from Biocell Biotech. Co., Ltd (Zhengzhou, China, <http://chinabiocell.biogo.net>) and stored in refrigerator at 4 °C. Bovine serum albumin (BSA), sodium borohydride ($NaBH_4$), sodium citrate and tetraethoxysilane (TEOS) were purchased from the Sinopharm Chemical Reagent Co., Ltd (Shanghai, China, <http://www.reagent168.cn>). Human immunoglobulin G (IgG) were obtained from Sigma Co. (<http://www.sigmaaldrich.com>). Reduced graphene oxide (purity $\geq 98\%$) (rGO) was purchased from Sinocarbon Materials Technology Co., Ltd (Taiyuan, Shangxi, <http://www.sinocarbon-cas.com>). Ferrocenecarboxylic acid (Fc), Azure A, (3-Aminopropyl) triethoxysilane (APTES), N-(3-Dimethylaminopropyl)-N-ethylcarbodiimide hydrochloride (EDC) and N-Hydroxysuccinimide (NHS) were purchased from Aladdin Reagent Co. (St. Louis, USA, <http://www.aladdin-e.com>). Chloroauric acid ($HAuCl_4 \cdot 4H_2O$) was obtained from Shanghai Chemical Reagent Co., Ltd. (Shanghai, China, <http://ccn.mofcom.gov.cn>). Phosphate buffer saline (PBS) with various pH values were prepared by mixing the stock solution of 0.1 M Na_2HPO_4 and 0.1 M NaH_2PO_4 . The washing buffer was pH 7.0 PBS containing 0.05 % (w/v) Tween (PBST). The clinical serum samples were from the clinical laboratory of the Yiji Shan Hospital (Wuhu, China). All solutions were prepared with twice-quartz-distilled water.

Apparatus

Electrochemical measurements were performed on a CHI 650C electrochemical analyzer (Shanghai Chenhua Instrument Co., China). The three-electrode system consisted of a platinum wire as the auxiliary electrode, a saturated calomel electrode (SCE) as the reference electrode and bare glassy carbon electrode (GCE) or modified electrode as the working electrode. Scanning electron microscope (SEM, S-4800, Hitachi, Japan), dynamic light scattering (DLS, 5022 F ALV/Laser Vertriebsgesellschaft m.b.H, Germany)

and energy dispersive x-ray spectrometer (EDS) were employed to investigate the various nanomaterial prepared.

Preparation of Si@Au NPs nanocomposites

Si NPs were synthesized according to the Stöber method with a slight modification [20]. Briefly, 4.0 mL TEOS was firstly added to a mixture containing 47.0 mL ethanol and 3.3 mL ammonium hydroxide under stirring and reacted for 24 h. Next, 0.3 mL APTES was added to functionalize the silica colloidal. After the solution was centrifugal treated, the product was dried at 50 °C for 6 h.

3.0 mL NaBH₄ (0.001 M) was slowly added to 20 mL HAuCl₄ (0.002 M) and reacted for a few minutes. Next, 2.0 mL sodium citrate (0.01 M) and 4.0 mL APTES-functionalized Si NPs (0.02 g APTES-functionalized Si NPs was suspended in 4.0 mL water) were added into solution above in sequence and reacted for 3 h under stirring. After the product was treated by centrifuging and washing, it was re-dispersed in 2.0 mL PBS. Thus, the product obtained was Si@Au NPs nanocomposite.

Preparation of two labels

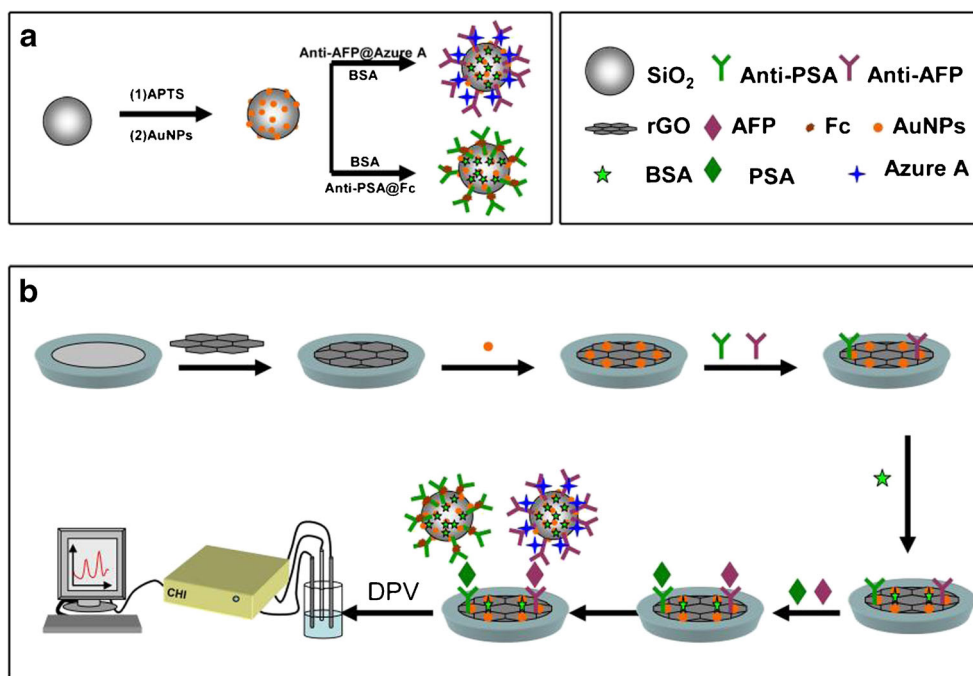
In this study, we synthesized two labels, one is Fc@Ab₂/Si@Au NPs bioconjugates and the other is Azure A@Ab₂/Si@Au NPs bioconjugates. Here, we described the preparation of the Fc@Ab₂/Si@Au NPs bioconjugates. Simply, 200 μL EDC (300 mM) and 200 μL NHS (100 mM) were first injected into 2.0 mL Fc (1.0 mg mL⁻¹) and reacted for 1 h.

After that, 150 μL anti-PSA (Ab₂) was injected into the solution above. After 24 h, the excessive Fc and coupling agent were removed by centrifuging. Thus, the product obtained was Fc@Ab₂. For further used, it was dispersed in 500 μL pH 7.4 PBS. Second, the Fc@Ab₂ solution was added into 1.0 mL Si@Au NPs nanocomposites and reacted for 12 h under stirring condition, next, 100 μL BSA was added to block all active sites. Subsequently, the solution was treated by centrifuging and washing, the product obtained was Fc@Ab₂/Si@Au NPs bioconjugates. In experiment, the product was need re-dispersed in 1.0 mL pH 7.4 PBS and stored at 4 °C for use. Similarly, Azure A@Ab₂/Si@Au NPs bioconjugates were preparation according to the similar procedures of the Fc@Ab₂/Si@Au NPs.

Fabrication protocol of the immunosensor

The fabrication protocol of the immunosensor is shown in Scheme 1. First, 5 μL rGO was dropped onto the surface of the pre-treated GCE (the treatment procedure is according to literature [21]) and dried in air. Subsequently, the electrode modified with rGO was immersed in 1.0 mg mL⁻¹ HAuCl₄ solution, and electrodeposited for 20 s at -0.20 V. During the process, the Au NPs was deposited on the surface of the rGO. Second, the electrode modified with Au NPs/rGO was immersed in the mixture containing two types of Ab₁ for 12 h at 4 °C for the immobilization of Ab₁. After washing with water, the modified electrode was incubated with 1 % BSA solution for 1 h at 37 °C. Thus, the immunosensor was obtained.

Scheme 1 Schematic representation of the fabrication procedure of the immunosensor



Electrochemical measurements

Before measurement, the immunosensor was incubated with the various concentrations of AFP and PSA or serum samples for 50 min at 37 °C. Then, it was incubated with the mixture containing redox-probes@Ab₂/Si@Au NPs nanocomposites for another 50 min at 37 °C. Finally, the immunosensor was transferred to 10 mL electrolytic cell with 3.0 mL pH 6.5 PBS solutions for electrochemical measurement. Before experiment, high-purity nitrogen was used for 10 min to remove oxygen of the solution, and a blanket of nitrogen was maintained during the measurements. DPV technique was employed to record the responsive signals from redox probes. The experiment parameters are listed as follows: initial potential, -0.8 V; final potential, 0.4 V; pulse amplitude, 0.05 V; pulse width, 0.25 s; sample interval, 0.002 s.

Results and discussion

Choice of materials

As is well known, graphene and carbon nanotubes have been used in sensing field for improving sensing performance due to their larger surface area and good conductivity. Carbon nanotubes-based immunosensors have been reported. For example, Lin's group [22] have reported an immunosensor for the CEA detection based on carbon nanotubes decorated with gold nanoclusters as sensing interface; Our groups [23] have reported a high sensitive immunosensor based on thionine-carbon nanotubes nanocomposite as sensing substrate, and HRP-carbon nanotubes as labels for the CEA detection. However, the functionalization of carbon nanotubes requires harsh condition and costs longer time. Because Si NPs are easily synthesized and functionalized, previously studies showed the Si NPs provide larger surface area for the signal tags and antibody immobilization, as a result, the immunosensor obtained had high sensitivity. Based on the advantages of Si NPs and graphene, we adopted rGO instead of carbon nanotubes as substrate in present work, and Si NPs were employed as carriers for immobilization of Au NPs, signal tags and antibodies. Based on this design, we hope that the immunosensor obtained had high sensitivity and selectivity for the multiple biomarkers detection.

Structure characterizations

The synthesized nanocomposites were investigated using SEM, DLS and EDS. Figure 1 showed the SEM image of Si NPs and Si@Au NPs nanocomposite. From Fig. 1a, it can be observed that the synthesized Si NPs exhibited a homogeneous structure. From Fig. 1c, it can be seen that Au NPs were dispersed onto the surface of Si NPs. The Si NPs provided a

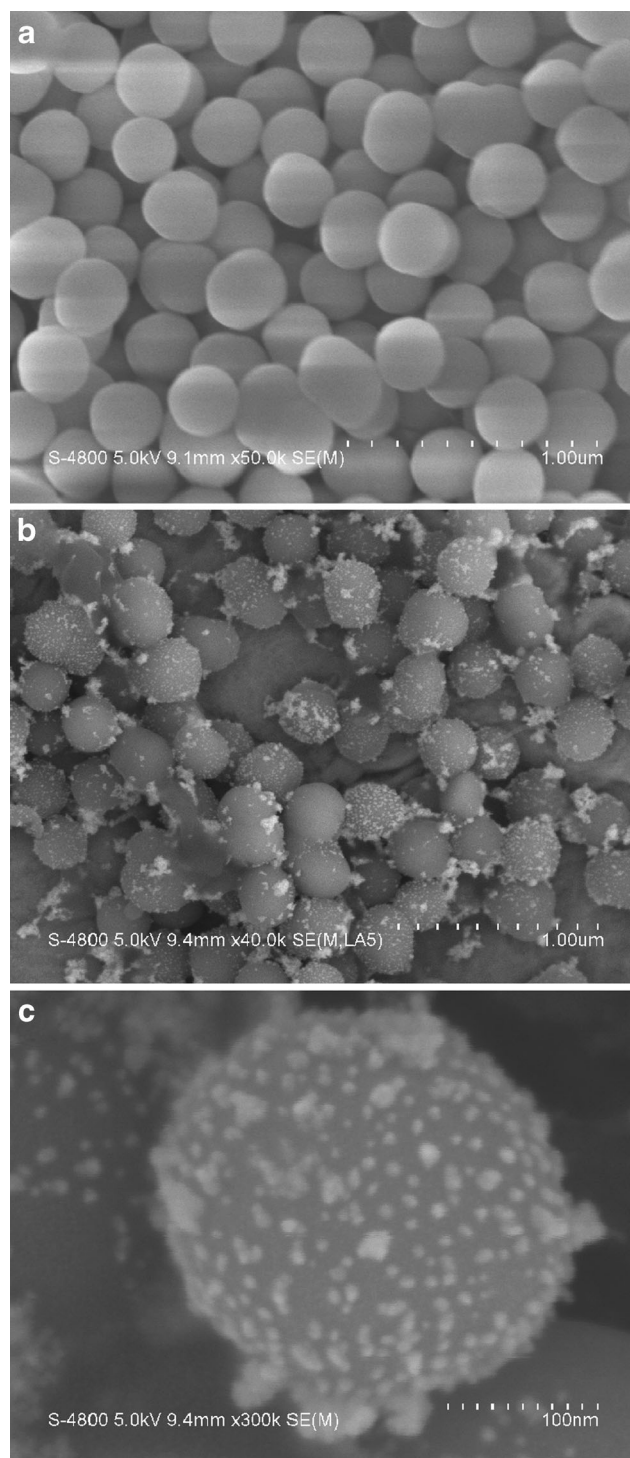


Fig. 1 SEM images of **a** Si NPs, **b** Si@Au NPs, **c** Si@Au NPs (at high magnification)

large surface area for amount of Au NPs immobilization. Therefore, the Si@Au NPs nanocomposite not only improved the immobilization of capture antibody, but also can improve the electron transfer rate due to good conductivity of Au NPs. In order to obtain the Si NPs particles size, DLS was employed to investigate and the particles size distribution

and results are shown in Fig. S1. The particles size was mainly distributed in range of 200–250 nm. EDS is employed to analyze the elemental compositions of Si@Au NPs nanocomposite (Seen Fig. S2). From Fig. S2, the signature peaks of Si, O and Au were clearly observed, indicating the Si@Au NPs nanocomposite was successfully prepared.

Similarly, the characterization of the rGO and rGO/Au NPs are shown in Fig S3. It can be observed that rGO showed the typical crumpled and flake structure, after electrodeposited in 1.0 mg mL^{-1} HAuCl₄ solution, Au NPs were distributed uniformly on the surface of rGO. EDS results confirmed the Au NPs existence on the surface of rGO (Seen Fig. 3SC).

Investigation the assembled process of immunosensor

Figure 2a shows the DPV results of the different assembled steps of the immunosensor in $1.0 \text{ mM} [\text{Fe}(\text{CN})_6]^{4-/3-}$ solution. The peak current clearly increased at rGO modified electrode (curve b) in contrast to the bare GCE (curve a). After the Au NPs were assembled onto the surface of rGO/GCE, the peak current increased clearly (curve c), indicating rGO and Au NPs have good conductivity. However, when the modified electrode was immobilized with anti-AFP and anti-PSA

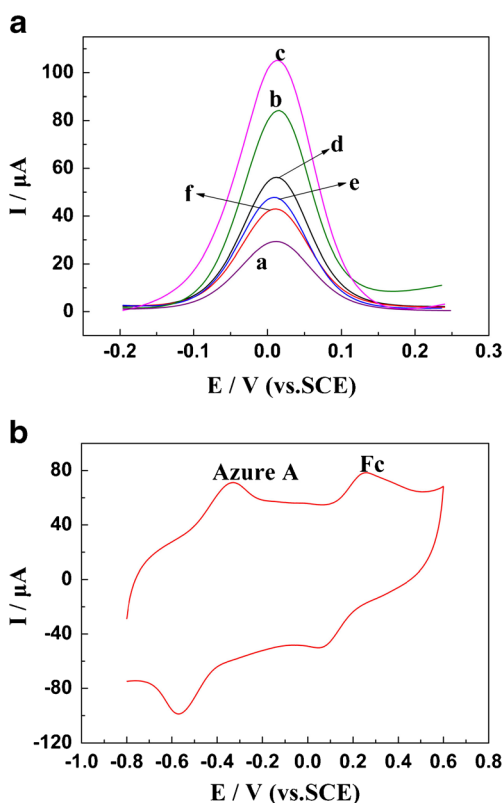


Fig. 2 a DPV responses of different assembled steps of the immunosensor in $1 \text{ mM} [\text{Fe}(\text{CN})_6]^{3-/4-}$ solution. (a) bare GCE, (b) rGO/GCE, (c) Au NPs/rGO/GCE, (d) Ab₁/Au NPs/rGO/GCE, (e) BSA/Ab₁/Au NPs/rGO/GCE, (f) antigens/BSA/Ab₁/Au NPs/rGO/GCE. b CVs of the immunosensor in pH 6.5 PBS in the presence of AFP and PSA antigens and Si@Au NPs/redox probes@Ab₂ nanocomposites

mixture (curve d) or blocked out with 1 % BSA (curve e), the peak currents clearly decreased due to the formation of the insulating layer from antibody or protein and blocks the electron transfer of $[\text{Fe}(\text{CN})_6]^{4-/3-}$ at electrode interface. When the modified electrode was employed to recognized antigens (curve f), the peak current decreased continuously. The reason is ascribed to the immunocomplex formation from the antigen-antibody. Figure 2b shows the cyclic voltammograms (CVs) of the immunosensor in presence of antigens and redox-probes@Ab₂/Si@Au NPs. From Fig. 2b, two couples of redox peaks corresponding to Fc and Azure A were observed in CVs, indicating two kinds of redox-probes were successfully attached onto the electrode surface via sandwich type immunoreaction. In this study, we also investigated the effect of Si@Au NPs and rGO on responsive signal, the results showed the responsive signal are obviously increased in presence of Si@Au NPs and rGO (Seen in Fig. S4), Therefore, we selected rGO as sensing substrate and Si@Au NPs as the immobilization of Ab₂ and redox –probes.

Optimization of experimental conditions

As is well known, the incubation time of antigen-antibody reaction and pH value greatly affects the immunosensor sensitivity. In this study, we investigated the effect of incubation time and pH on response signal. All results are shown in Fig. S5. From Fig. S5, it can be observed that the following experimental conditions were found to give best results: (a) A sample pH value of 6.5; (b) an incubation time of 50 min.

Investigation of the nonspecific adsorption and cross-reactivity of immunoassay

In this study, we had investigated the nonspecific adsorption of immunosensor with and without BSA elimination. The

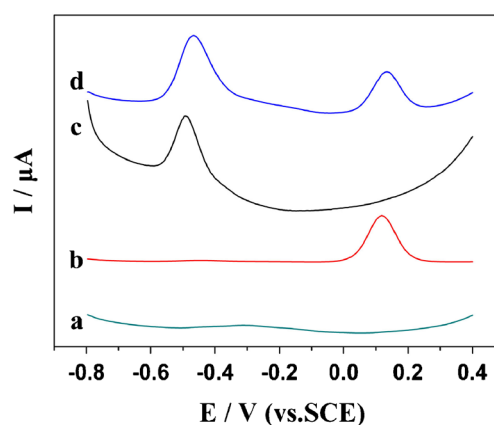


Fig. 3 DPV responses of immunosensor in presence of various conditions a 0 ng mL^{-1} PSA and 0 ng mL^{-1} AFP solution, b 1 ng mL^{-1} PSA, c 10 ng mL^{-1} AFP and d 1 ng mL^{-1} PSA and 10 ng mL^{-1} AFP solution with redox-probes@Ab₂/Si@Au NPs nanocomposites as labels

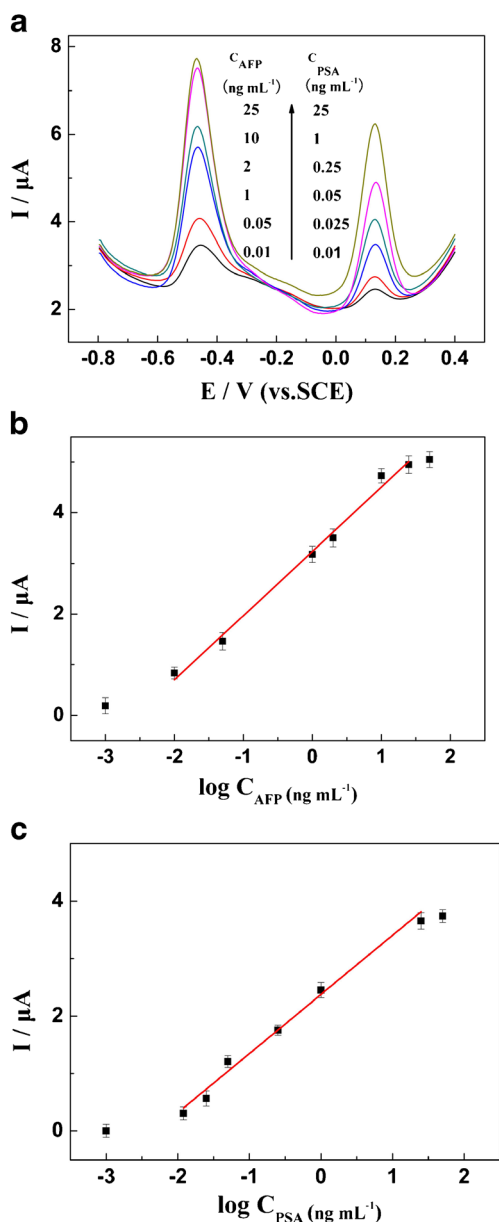


Fig. 4 **a** DPV responses of the immunosensor in presence of different concentrations of AFP and PSA. **b, c** Calibration curves between peak current and the logarithm of the biomarkers concentration. The error bars stand for the standard deviations of different parallel samples at each target concentration

results are shown in Fig. S6. The results showed the immunosensor need BSA to block out active sites. The investigation of the nonspecific adsorption and cross-reactivity of immunosensor were carried out in absence and presence of tumor biomarkers, and results are shown in Fig. 3. It can be observed that no signal was obtained when the immunosensor was employed to detect the solution without PSA and AFP, indicating nonspecific adsorption of the immunosensor was negligible (Seen curve a). In order to estimate the cross-reactivity of the immunoassay, the immunosensor was employed to detect various solutions in the presence of PSA or AFP alone and both coexist. The results obtained were different completely. Two well-resolved oxidation peaks, one is at -0.48 V vs. SCE (corresponding to Azure A) and other is at $+0.12$ V vs. SCE (corresponding to Fc) can be observed in DPV curves and the peak potential difference was about 600 mV in presence of PSA and AFP (Seen cure d), indicating the responsive signal from Azure A and Fc according to two biomarkers can be appeared alone and don't be overlapped. The peak currents different is 1.4 % for PSA in absence and presence of AFP and 0.7 % for AFP in absence and presence of PSA, indicating that the cross-reactivity from the two biomarkers is negligible.

Analytical performance

The analytical performance of immunosensor was evaluated by simultaneous detecting various concentrations of AFP and PSA using DPV technology, and the results are shown in Fig. 4. The peak currents of both Azure A and Fc were simultaneously increased with increasing concentration of AFP and PSA, and a good calibration curves between peak currents and the logarithmic of biomarkers concentration were obtained in the range of 0.01 – 25 $ng mL^{-1}$ for AFP and 0.012 – 25 $ng mL^{-1}$ for PSA. For AFP, the linear regression equation was $I (\mu A) = 3.29 + 1.27 \log C$ (unit of C is $ng mL^{-1}$) and the correlation coefficients was 0.9950; For PSA, the linear regression equation was $I (\mu A) = 2.39 + 1.03 \log C$ (unit of C is $ng mL^{-1}$) and the correlation coefficients was 0.9900. The detection limits of AFP and PSA were 3.3 $pg mL^{-1}$ and 4.0 $pg mL^{-1}$ (at a signal to noise ratio of 3), respectively. Compared with some

Table 1 Analytical performance of several electrochemical immunosensors

	Line arrange ($ng mL^{-1}$)		Detection limit ($ng mL^{-1}$)		References		
Quantum dots coated silica nanoparticles as probes	CEA	0.05–25 IgG	0.05–40	CEA 0.005	IgG	0.005	[15]
A branched electrode based immunosensor	CEA	0.5–80 AFP	0.5–50	CEA 0.05	AFP	0.1	[24]
Reduced graphene oxide tetraethylene pentamine as electrode materials	CEA	0.05–20 SCCA	0.03–20	CEA 0.013	SCCA	0.01	[25]
Multi-functionalized onion-like mesoporous graphene sheets	PSA	0.01–50 fPSA	0.01–50	PSA 0.0067	fPSA	0.0034	[26]
This work	AFP	0.01–25 PSA	0.01–25	AFP 0.0033	PSA	0.004	

recently published work (Seen in Table 1), the immunosensor exhibits wide linear range and lower detection limit.

Reproducibility, selectivity and stability of the immunosensor

In this study, the reproducibility of immunosensor was evaluated by intra and inter-assay precision. The intra-assay precision was obtained by detecting three different concentrations of AFP (0.01, 0.05 and 25 ng mL⁻¹) and PSA (0.05, 0.25 and 1 ng mL⁻¹) mixed antigens using identical immunosensor and recorded their peak currents. The variation coefficient obtained ($n=5$) were 3.5, 4.8 and 2.6 % for 0.01, 0.05 and 25 ng mL⁻¹AFP, and 4.9, 7.8 and 4.0 % for 0.05, 0.25 and 1 ng mL⁻¹ PSA, respectively. The inter-assay precision was investigated by measuring three different concentrations of mixed antigens using five immunosensors fabricated under the same condition. The variation coefficient ($n=5$) were 4.0, 5.5 and 4.4 % for 0.01, 0.05 and 25 ng mL⁻¹ AFP; 3.5, 4.3 and 5.0 % for 0.05, 0.25 and 1 ng mL⁻¹ PSA, indicating the immunosensor possesses good reproducibility.

The selectivity of the immunosensor was evaluated using CEA, HCG and IgG as the possible interference substance and recorded their peak currents in presence of 1 ng mL⁻¹ AFP and 1 ng mL⁻¹ PSA alone and co-exist with 100 ng mL⁻¹ other interfere substance. The results obtained are shown in Fig. S7. It can be observed that the signal intensities corresponding to AFP and PSA were almost kept a constant, indicating the immunosensor had good selectivity.

The stability of the immunosensor was also examined in presence of 1 ng mL⁻¹ AFP. The response value of the immunosensor maintains 98.6, 96.2, 95.8, 94.7, 93.5 and 91.6 % of initial value after 3, 6, 9, 12, 15 and 20 days preservation, which shows that the immunosensor exhibits good stability.

Real samples analysis

To investigate the performance of the immunosensor in clinical analysis, recovery experiments were performed by spiking different concentrations (AFP and PSA) standards into the blank serum specimens, and detect their content using the immunosensor. Simply, 20 μ L serum samples from normal human (Yiji Shan Hospital provided) was injected into 3.0 mL pH 6.5 PBS. Then, different concentrations of AFP and PSA were added into the solution above. The detection procedure is according to the electrochemical measurement, and the results obtained are shown in Table S1, the recovery obtained were within 96.0–107.2 % for PSA and 100.9–105.8 % for AFP, indicating the immunosensor can be applied to simultaneously detect AFP and PSA in human serum.

Conclusions

In summary, a simple and sensitive immunosensor for the simultaneous detection of AFP and PSA has been described using Azure A and Fc as labels. The experimental results show that the immunosensor exhibits wide linear response range and high sensitivity. In particular, the immunosensor provides a promising application in clinical analysis.

Acknowledgments This work was financially supported by the National Natural Science Foundation of China (No. 20675002). This work is also supported by the Special Foundation for Excellent Doctoral Fostering of Anhui Normal University Organic Chemistry (No. 003061425).

References

1. Qu B, Chu X, Shen GL, Yu RQ (2008) A novel electrochemical immunosensor based on colabeled silica nanoparticles for determination of total prostate specific antigen in human serum. *Talanta* 76: 785–790
2. Tian JN, Huang JL, Zhao YC, Zhao SL (2012) Electrochemical immunosensor for prostate-specific antigen using a glassy carbon electrode modified with a nanocomposite containing gold nanoparticles supported with starch-functionalized multi-walled carbon nanotubes. *Microchim Acta* 178:81–88
3. Xu X, Ying YB, Li YB (2012) One-step and label-free detection of alpha-fetoprotein based on aggregation of gold nanorods. *Sensors Actuators B* 175:194–200
4. Liu N, Ma ZF (2014) Au-ionic liquid functionalized reduced graphene oxide immunosensing platform for simultaneous electrochemical detection of multiple analytes. *Biosens Bioelectron* 51: 184–190
5. Lin JH, Zhang HH, Niu SY (2015) Simultaneous determination of carcinoembryonic antigen and α -fetoprotein using an ITO immunoelectrode modified with gold nanoparticles and mesoporous silica. *Microchim Acta* 182:719–726
6. Zhang Y, Dai WJ, Liu F, Li L, Li M, Ge SG, Yan M, Yu JH (2013) Ultrasensitive electrochemiluminescent immunosensor based on dual signal amplification strategy of gold nanoparticles-dotted graphene composites and CdTe quantum dots coated silica nanoparticles. *Anal Bioanal Chem* 405:4921–4929
7. Zhang F, Mao L, Zhu MQ (2014) Ultrasensitive immunoassay for free prostate-specific antigen based on ferrocenecarboxylate enhanced cathodic electrochemiluminescence of peroxydisulfate. *Microchim Acta* 181:1285–1291
8. Wu J, Fu ZF, Yan F, Ju HX (2007) Biomedical and clinical applications of immunoassays and immunosensors for tumor markers. *TrAC Trends Anal Chem* 26:679–688
9. Du D, Zou ZX, Shin YS, Wang J, Wu H, Engelhard MH, Liu J, Aksay IA, Lin YH (2010) Sensitive immunosensor for cancer biomarker based on dual signal amplification strategy of graphene sheets and multienzyme functionalized carbon nanospheres. *Anal Chem* 82:2989–2995
10. Hansen JA, Wang J, Kawde AN, Xiang Y, Gothelf KV, Collins G (2006) Quantum dot/aptamer-based ultrasensitive multianalyte electrochemical biosensor. *J Am Chem Soc* 128:2228–2229
11. Liu J, Lee JH, Lu Y (2007) Quantum dot encoding of aptamer-linked nanostructures for one-pot simultaneous detection of multiple analytes. *Anal Chem* 79:4120–4125
12. Tang DP, Hou L, Niessner R, Xu MD, Gao ZQ, Knopp D (2013) Multiplexed electrochemical immunoassay of biomarkers using

- metal sulfide quantum dot nanolabels and trifunctionalized magnetic beads. *Anal Chem* 46:37–43
13. Yan J, Estévez MC, Smith JE, Wang KM, He XX, Wang L, Tan W (2007) Dye-doped nanoparticles for bioanalysis. *Nano Today* 2:44–50
 14. Li Y, Yuan R, Chai YQ, Zhuo Y, Su HL, Zhang YX (2014) Horseradish peroxidase-loaded nanospheres attached to hollow gold nanoparticles as signal enhancers in an ultrasensitive immunoassay for alpha-fetoprotein. *Microchim Acta* 181:679–685
 15. Qian J, Dai HC, Pan XH, Liu SQ (2011) Simultaneous detection of dual proteins using quantum dots coated silica nanoparticles as labels. *Biosens Bioelectron* 28:314–319
 16. Tang J, Tang DP, Niessner R, Chen GN, Knopp D (2011) Magneto-controlled graphene immunosensing platform for simultaneous multiplexed electrochemical immunoassay using distinguishable signal tags. *Anal Chem* 83:5407–5414
 17. Ji XL, Liu ZM, Liu N, Ma ZF (2014) A label-free immunosensor based on graphene nanocomposites for simultaneous multiplexed electrochemical determination of tumor markers. *Biosens Bioelectron* 53:160–166
 18. Zhu Q, Chai YQ, Yuan R, Zhuo Y, Han J, Li Y, Liao N (2013) Amperometric immunosensor for simultaneous detection of three analytes in one interface using dual functionalized graphene sheets integrated with redox-probes as tracer matrixes. *Biosens Bioelectron* 43:440–445
 19. Feng DX, Li LH, Han XW, Fang X, Li XZ, Zhang YZ (2014) Simultaneous electrochemical detection of multiple tumor markers using functionalized graphene nanocomposites as non-enzymatic labels. *Sensors Actuators B* 201:360–368
 20. Stöber W, Fink A, Bohn E (1968) Controlled growth of monodisperse silica spheres in the micron size range. *Colloid Interface Sci* 26:62–69
 21. Wang J, Shi AQ, Fang X, Han XW, Zhang YZ (2014) Ultrasensitive electrochemical supersandwich DNA biosensor using a glassy carbon electrode modified with gold particle decorated sheets of graphene oxide. *Microchim Acta* 181:935–940
 22. Gao X, Zhang YM, Chen H, Chen ZC, Lin XF (2011) Amperometric immunosensor for carcinoembryonic antigen detection with carbon nanotube-based film decorated with gold nanoclusters. *Anal Biochem* 414:70–76
 23. Feng DX, Li LH, Fang X, Han XW, Zhang YZ (2014) Dual signal amplification of horseradish peroxidase functionalized nanocomposites as trace label for the electrochemical detection of carcinoembryonic antigen. *Electrochim Acta* 127:334–341
 24. Kong FY, Xu BY, Du Y, Xu JJ, Chen HY (2013) A branched electrode based electrochemical platform: towards new label-free and reagentless simultaneous detection of two biomarkers. *Chem Commun* 49:1052–1054
 25. Wu D, Guo AP, Guo ZK, Xie LL, Wei Q, Du B (2014) Simultaneous electrochemical detection of cervical cancer markers using reduced graphene oxide-tetraethylene pentamine as electrode materials and distinguishable redox probes as labels. *Biosens Bioelectron* 54:634–639
 26. Han J, Zhuo Y, Chai YQ, Yuan R, Zhang W, Zhu Q (2012) Simultaneous electrochemical detection of multiple tumor markers based on dual catalysis amplification of multi-functionalized onion-like mesoporous graphene sheets. *Anal Chim Acta* 746:70–76